

THEMIS observations of ULF wave excitation in the nightside plasma sheet during sudden impulse events

Q. Q. Shi,^{1,2} M. Hartinger,¹ V. Angelopoulos,¹ Q.-G. Zong,³ X.-Z. Zhou,¹ X.-Y. Zhou,^{1,6} A. Kellerman,¹ A. M. Tian,² J. Weygand,¹ S. Y. Fu,³ Z. Y. Pu,³ J. Raeder,⁴ Y. S. Ge,⁴ Y. F. Wang,³ H. Zhang,⁵ and Z. H. Yao³

Received 5 June 2012; revised 31 October 2012; accepted 21 November 2012; published 24 January 2013.

[1] Sudden impulses (SIs) are an important source of ultra low frequency (ULF) wave activity throughout the Earth's magnetosphere. Most SI-induced ULF wave events have been reported in the dayside magnetosphere; it is not clear when and how SIs drive ULF wave activity in the nightside plasma sheet. We examined the ULF response of the nightside plasma sheet to SIs using an ensemble of 13 SI events observed by THEMIS (Timed History of Events and Macroscale Interactions during Substorms) satellites (probes). Only three of these events resulted in ULF wave activity. The periods of the waves are found to be 3.3, 6.0, and 7.6 min. East-west magnetic and radial electric field perturbations, which typically indicate the toroidal mode, are found to be stronger and can have phase relationships consistent with standing waves. Our results suggest that the two largest-amplitude ULF responses to SIs in the nightside plasma sheet are tailward-moving vortices, which have previously been reported, and the dynamic response of cross-tail currents in the magnetotail to maintain force balance with the solar wind, which has not previously been reported as a ULF wave driver. Both mechanisms could potentially drive standing Alfvén waves (toroidal modes) observed via the field-line resonance mechanism. Furthermore, both involve frequency selection and a preference for certain driving conditions that can explain the small number of ULF wave events associated with SIs in the nightside plasma sheet.

Citation: Shi, Q. Q., et al. (2013), THEMIS observations of ULF wave excitation in the nightside plasma sheet during sudden impulse events, *J. Geophys. Res. Space Physics*, 118, 284–298, doi:10.1029/2012JA017984.

1. Introduction

[2] Ultra low frequency (ULF) waves play an important role in energy transport from the solar wind into the magnetosphere [e.g., *Glassmeier et al.*, 1999; *McPherron*, 2005; *Kivelson*, 2006; and references therein]. For example, they modulate auroral activity [e.g., *Greenwald and Walker*, 1980; *Samson et al.*, 1996], heat the ionosphere [e.g., *Glassmeier et al.*,

1999; *Rae et al.*, 2007; *Hartinger et al.*, 2011], and interact with magnetospheric particles [e.g., *Southwood and Kivelson*, 1981; *Baumjohann et al.*, 1983; *Zong et al.*, 2009]. One of the most important mechanisms for ULF wave energy transfer is resonant coupling between fast and shear Alfvén wave modes known as field-line resonance (FLR) [e.g., *Southwood*, 1974].

[3] Rapid compressions of the Earth's magnetosphere, sudden impulses (SIs) are typically caused by extremely fast increase of solar wind dynamic pressure often associated with interplanetary shocks. SIs can drive different types of ULF activity, including shear Alfvén waves and tailward moving vortices associated with magnetopause surface waves [*Sibeck*, 1990; *Southwood and Kivelson*, 1990]. Most in situ observations of ULF waves induced by sudden impulses have been on the dayside [*Kaufmann and Walker*, 1974; *Nopper et al.*, 1982; *Wilken et al.*, 1982; *Baumjohann et al.*, 1984; *Wedeken et al.*, 1984; *Cahill et al.*, 1990; *Sarris et al.*, 2010; *Hartinger et al.*, 2011]. For example, using recent THEMIS multi-satellite data, *Sarris et al.* [2010] studied temporal and spatial characteristics of FLRs in the dayside magnetosphere. *Eriksson et al.* [2006] found that solar wind pressure enhancements can excite waveguide modes that can couple to toroidal and poloidal mode waves in the dayside magnetosphere.

[4] There have been a few studies of ULF wave activity on the nightside which did not specifically examine the

¹Earth and Space Sciences Department, University of California, Los Angeles, California, USA.

²Shandong Provincial Key Laboratory of Optical Astronomy and Solar-Terrestrial Environment, School of Space Science and Physics, Shandong University, Weihai, China.

³School of Earth and Space Sciences, Peking University, Beijing, China.

⁴Space Science Center and Physics Department, University of New Hampshire, Durham, New Hampshire, USA.

⁵Physics Department and Geophysical Institute, University of Alaska Fairbanks, Fairbanks, Alaska, USA.

⁶On-leave from JPL.

Corresponding author: Q. Q. Shi, Shandong Provincial Key Laboratory of Optical Astronomy and Solar-Terrestrial Environment, School of Space Science and Physics, Shandong University, Weihai, China. (sqq@pku.edu.cn)

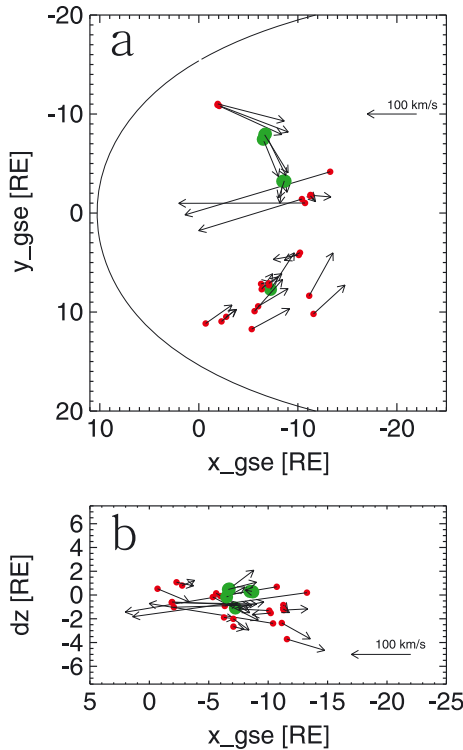


Figure 1. Position of the THEMIS probes for events in which shock or dynamic pressure enhancement were observed in the solar wind and sudden impulses were observed by THEMIS in the magnetotail. Events marked by green-filled circles are studied in this paper. Arrows indicate the initial velocity perturbation induced by the sudden impulse (a) in the GSE xy plane and (b) in the GSM x - dz plane, where dz is the distance to the neutral sheet using a model [Hammond *et al.*, 1994]. The curve in Figure 1a is the nominal magnetopause location, calculated using Shue *et al.*'s [1998] model with $Dp = 2$ nPa and $Bz = 1$ nT.

response to SIs [e.g., Sarafopoulos and Sarris, 1994; Zheng *et al.*, 2006; Zhang *et al.*, 2010; Tian *et al.*, 2012]. For example, Sarafopoulos and Sarris [1994] presented three case studies of ULF wave events in the magnetotail that were consistent with a tailward-moving vortex associated with a magnetopause surface wave. Zheng *et al.* [2006] reported a low frequency FLR event in the mid-tail using coordinated in situ and ground-based observations. Tian *et al.* [2012] observed ULF waves in the magnetotail and interpreted them as FLRs driven by cavity/waveguide modes in the nightside outer magnetosphere after a period of long-lasting northward interplanetary magnetic field (IMF). Yao *et al.* [2010] reported oscillations in the ULF frequency range on the nightside following SI events, but they did not analyze the wave properties or provide a wave excitation mechanism.

[5] The ULF response of the magnetotail to SIs, an important driver of ULF wave activity in the dayside magnetosphere, remains an open question. In this paper, we examine the response of the nightside magnetosphere to 13 SI events and find only three cases with ULF wave activity. In section 2, we describe how we selected these three ULF wave events and show data from each event; all three include observations in the solar wind and in the nightside magnetosphere (at a

geocentric distance of about 9–11 Re). In section 3, we compare our observations with several mechanisms that could excite ULF waves during SI events, showing that tailward-moving vortices and dynamic force balance between the solar wind and magnetotail are most consistent with the observations. We summarize our results in the last section.

2. Observation Overview

[6] We use data from the five satellite THEMIS mission [Angelopoulos, 2008]. Solar wind and IMF data are from the Wind satellite [Farrell *et al.*, 1995; Gloeckler *et al.*, 1995], Cluster satellites [Balogh *et al.*, 2001; Reme *et al.*, 2001], and THEMIS satellites. Three-second spin resolution data from a fluxgate magnetometer (FGM) [Auster *et al.*, 2008] and an ion and electron electrostatic analyzer (ESA) [McFadden *et al.*, 2008] onboard THEMIS are used.

[7] We examined 13 SI events associated with interplanetary shocks or solar wind dynamic pressure enhancements during which at least one THEMIS probe was in the magnetotail (positions shown in Figure 1); 30 observations are associated with these SI events, because multiple THEMIS probes were in the tail in many events. Among the 13 events, we found three in which at least one THEMIS probe observed clear wave activity (one event was in the duskside, one in the dawnside, and one near midnight, as marked in Figure 1). The arrows in the plots indicate the peak velocity during the first 1/2 waveform, which show that most cases had an initial response although not all cases have ULF wave observations. From Figure 1a, we find that most arrows point to the tail and the $y=0$ plane, consistent with compression due to shock/dynamic pressure.

[8] We identified clear wave activity using two techniques: an index representing the duration of wave activity in the frequency band of peak power spectral density (period between 1 and 15 min) and visual inspection.

[9] To obtain the index value for each event, we first performed a wavelet transform on the x component of the velocity perturbation (from ESA data). Next, we selected the frequency band (between ~ 1 and 17 mHz) with peak power spectral density during the SI. Finally, we recorded the length of time in this frequency band for the power spectral density to reduce to half of its original value; the index is this time length normalized to the wave period (consistent with the selected frequency band). This index defines how many periods before the wave at the frequency with peak power damps to half of the beginning value.

[10] Ideally, this index is directly related to the duration of wave activity. To verify this, we visually inspected velocity traces for each event, finding that events with higher indexes had wave activity of longer duration; these events also typically had larger amplitude and more monochromatic wave activity. We conclude that this index can be used to automatically identify ULF wave events and separate them quantitatively from weak or transient responses to SIs. In one or two (e.g., 3 March 2009) of the 30 total observations, visual inspection showed that the index was not a good measure of wave activity duration or clarity, owing to the low time resolution of the wavelet analysis at low frequencies.

[11] The indices of all the events are listed in Table 1. The three events with very clear wave activity (29 March 2011, 11 April 2010, and 24 April 2009) had high index values

Table 1. The SI Events at the Magnetotail and the Clear Wave Index

Start time	S/C	Index
28 May 2008/02:27:00	d	0.9
14 January 2009/01:29:30	c	1.8
03 March 2009/06:06:20	a	4.3
24 April 2009/00:57:00	b	1.2
24 April 2009/00:57:00	c	0.6
24 April 2009/00:55:00	d	2.5
24 April 2009/00:54:00	e	1.4
28 May 2009/05:22:00	c	1.0
28 May 2009/05:21:40	d	0.9
28 May 2009/05:21:40	e	1.0
20 June 2009/04:52:30	d	0.8
20 June 2009/04:52:30	e	1.2
05 April 2010/08:28:40	a	1.3
05 April 2010/08:30:00	d	1.4
05 April 2010/08:29:40	e	1.5
11 April 2010/13:05:50	a	2.8
11 April 2010/13:05:00	d	3.8
11 April 2010/13:05:50	e	2.1
14 February 2011/15:58:00	a	1.6
14 February 2011/15:58:00	d	1.6
14 February 2011/15:58:00	e	1.6
29 March 2011/16:04:10	a	2.7
29 March 2011/16:04:00	d	3.1
29 March 2011/16:04:00	e	3.2
18 April 2011/06:57:30	a	1.0
10 June 2011/08:56:30	d	2.0
10 June 2011/08:52:00	e	1.1
17 June 2011/02:42:30	a	2.1
17 June 2011/02:42:30	d	1.1
17 June 2011/02:42:30	e	1.1

relative to other events (for at least one THEMIS probe observations) and were the easiest to identify as ULF wave events during visual inspection. Figure 1b shows that in these three cases the probes were close to the neutral sheet. In this section, we will describe the observational features of these three events.

2.1. The 29 March 2011 Event in the Dawn Flank Magnetotail

[12] On 29 March 2011 at $\sim 15:50$ UT, THEMIS B and C were in the solar wind at $(36.4, -42.4, -11.7)$ Re and $(26.3, -50.1, -15.5)$ Re, respectively, both in GSM coordinates. Figure 2 shows THEMIS C observations in the solar wind. At $\sim 15:55$ UT an interplanetary shock was observed and the solar wind dynamic pressure increased from 0.6 to 1.4 nPa. The shock normal is along $(-0.94, -0.05, 0.35)$ calculated from mixed coplanarity theory [Abraham-Shrauner, 1972] in GSM coordinates. We can get the shock velocity along the normal based on mass flux conservation, which is 414 km/s. Normal and velocity can be confirmed with an error of $\sim 4\%$ by the timing of THEMIS B and C.

[13] At about 16:02 UT THEMIS D was in the magnetotail at approximately $(-6.74, -8.91, 0.96)$ Re in GSM coordinates ($R \sim 11.21$ Re), with THEMIS A and E nearby. All three probes observed magnetotail compression during the shock passage, or SI. Figure 3 shows THEMIS D observations. Immediately after the sudden impulse, a clear quasi-sinusoidal wave signature with a period of ~ 6 min was found; it lasted at least half an hour, damping gradually. Magnetic field perturbations with similar periods were also seen, although they were not as clear as the velocity data.

[14] Figure 4 shows band-pass-filtered (2.77 ± 1 mHz) magnetic field and electric field (obtained from $\mathbf{V} \times \mathbf{B}$) data in a field-aligned coordinate system [e.g., *Hartinger et al.*, 2011] in which y points eastward, z is along the background magnetic field (direction obtained from low pass-filtered data, frequency < 0.5 mHz), and x completes the orthogonal set pointing approximately radially outward.

[15] Perturbations in Ex and By are typically associated with toroidal modes, or Alfvén waves with low azimuthal wave number; perturbations in Ey and Bx are associated with poloidal modes or Alfvén waves with high azimuthal wave number [e.g., *Dungey*, 1954, 1963; *Southwood and Hughes*, 1983]. The compressional component Bz can be associated with fast mode waves or poloidal mode Alfvén waves. Perturbations associated with the toroidal mode are stronger for this case. After an initial transient associated with the SI, the phase difference between the magnetic and electric field, shown in Figure 4e, is consistent with standing wave activity, as indicated by the 90° phase difference between Ex and By . The standing property of the transverse wave activity suggests that energy from compression of the magnetosphere was converted to standing Alfvén waves via field line resonance (FLR) [Southwood, 1974]. THEMIS A and E, which were close to THEMIS D (THEMIS A had a z separation of ~ 0.8 Re), also observed standing Alfvén wave activity (toroidal mode).

2.2. The 11 April 2010 Event in the Central Magnetotail

[16] Figure 5 shows THEMIS B observations in the solar wind on 11 April, 2010. At $\sim 12:57$ UT an interplanetary shock front was encountered by THEMIS B. The dynamic pressure changed from 0.6 to 1.5 nPa after the shock, which is very similar to the 29 March 2011 event. From the mixed coplanarity method of the shock, we can get the shock normal, which is confirmed by the Timing method [Russell *et al.*, 1983] for multiple spacecraft in the solar wind from Cluster magnetic field data. The shock normal is along $(-0.96, 0.27, -0.03)$ GSM, with a propagation speed of 363.3 km/s. Normal and velocity can be confirmed by the timing of THEMIS B in $(45.2, 35.9, 4.4)$ GSM and C at $(-125.5, -54.3, -24.5)$ GSM in the solar wind with a difference of 8%.

[17] At $\sim 13:04:25$ THEMIS A, D, and E (with ~ 0.8 Re separations) observed the SI followed by the wave with a period of 3.3 min, as seen clearly from the ion velocity data at approximately $(-8.49, -3.71, 1.78)$ Re (Figure 6). Figure 7 indicates large amplitude perturbations in the components associated with the toroidal mode (Ex, by), but the phase difference is not stable at a value close to 90° , as in the previous event. This could be because standing Alfvén waves are heavily damped in this region. If the wave is heavily damped, the main observation would be the transient response to the SI, which would not be effectively captured by the band pass filter (the result would be an unstable phase difference which is not physically meaningful).

2.3. The 24 April 2009 Event in the Dusk Flank Magnetotail

[18] For this case, the Wind satellite, which was in the solar wind, detected a shock (see Figure 8) with a dynamic pressure increase from ~ 0.7 to 1.7 nPa. THEMIS D in the

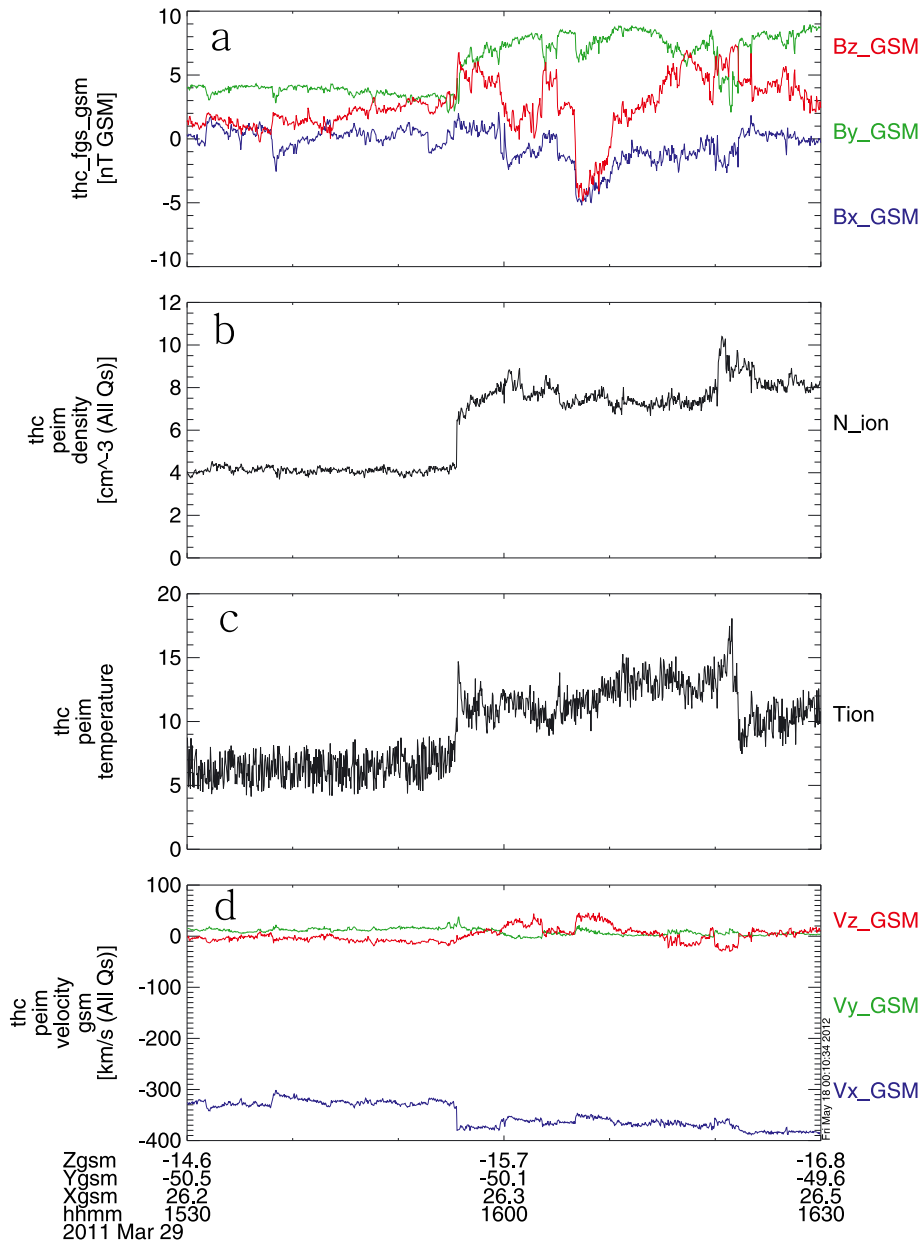


Figure 2. THEMIS C observations in the solar wind on 29 March 2011. (a) Magnetic field, (b) ion density, (c) ion temperature, and (d) ion velocity.

dusk magnetotail observed clear wave activity periods of ~ 7.6 min after the SI at 00:53 UT, as shown in Figure 9. E_x and b_y have the largest perturbations and a phase relationship indicating standing wave activity (Figure 10). Note that THEMIS E, which was located ~ 1 Re closer to the Earth, observed oscillations with much smaller amplitude than observed by THEMIS D. This difference was also evident in the ULF wave index for each observation, 2.5 for THEMIS D and 1.4 for THEMIS E.

3. Discussion

[19] We examined 13 SI events associated with interplanetary shocks or solar wind dynamic pressure enhancements, finding three in which ULF waves were excited in the magnetotail (Figure 1). In two cases, after an initial transient,

standing Alfvén waves consistent with toroidal modes were excited; in the other case, standing Alfvén waves may have been excited but were heavily damped. In at least one of these three cases, THEMIS probes located at different positions in the magnetotail did not observe clear ULF wave activity, suggesting that the wave activity might be localized. In the other 10 SI events, clear wave activity, as determined by visual inspection and a ULF wave index defined in section 2, was not observed by any THEMIS probes. *Lui and Cheng* [2001] calculated the FLR (standing Alfvén wave) frequency based on the Earth's dipole field and in their results, when $R=11.4$ Re, the frequency of the odd mode is 5.58 mHz. This is close to but higher than our observations, as expected for an un-stretched dipole field. *Rankin et al.* [2000] provide an equation for the number density along the field line and then use an empirical model with a

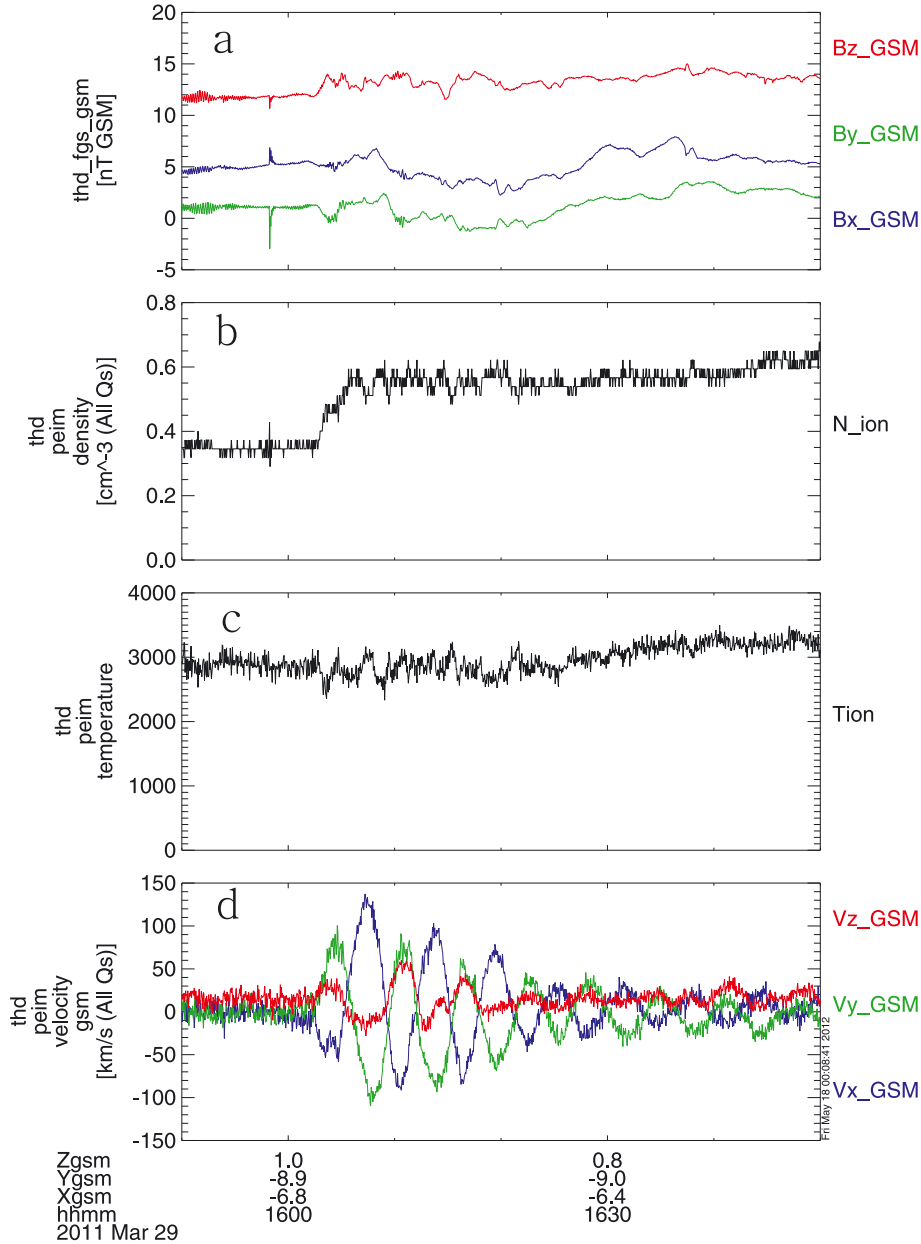


Figure 3. THEMIS D observations of the ULF wave on 29 March 2011. Format is the same as in Figure 2.

stretched field (T96) to compute the standing Alfvén wave frequencies in a cold plasma. For the third event, we calculated the field line resonance frequency using their model assuming the density in the equatorial plane is 1 n/cm^3 and obtain the toroidal frequency of the fundamental mode to be 3.4 mHz . This is close to the observations for events 1 and 3 and within the uncertainty expected for these model frequencies [e.g., *Berube et al.*, 2006]. These model comparisons are additional evidence that standing Alfvén waves, possibly generated by FLR, were observed. In events 1 and 3, the probes were close to the location where the field line resonance condition was met (driving frequency matches the local resonance frequency), and phase differences between the electric and magnetic field perturbations

consistent with standing Alfvén waves were observed. In event 2, the probe was likely further from the resonance location and observed perturbations consistent with heavily damped standing Alfvén waves.

[20] In this section, we discuss several possible mechanisms for ULF wave excitation in these events.

[21] 1. Surface waves at the magnetopause driven by the Kelvin-Helmholtz instability
 Significant shear flows in the magnetosheath can make the magnetopause unstable to the growth of surface waves; these surface waves can in turn couple to standing Alfvén waves via FLR inside the magnetosphere [*Chen and Hasegawa*, 1974; *Southwood*, 1974]. For shocks or pressure pulses impinging on the magnetosphere in our study, a

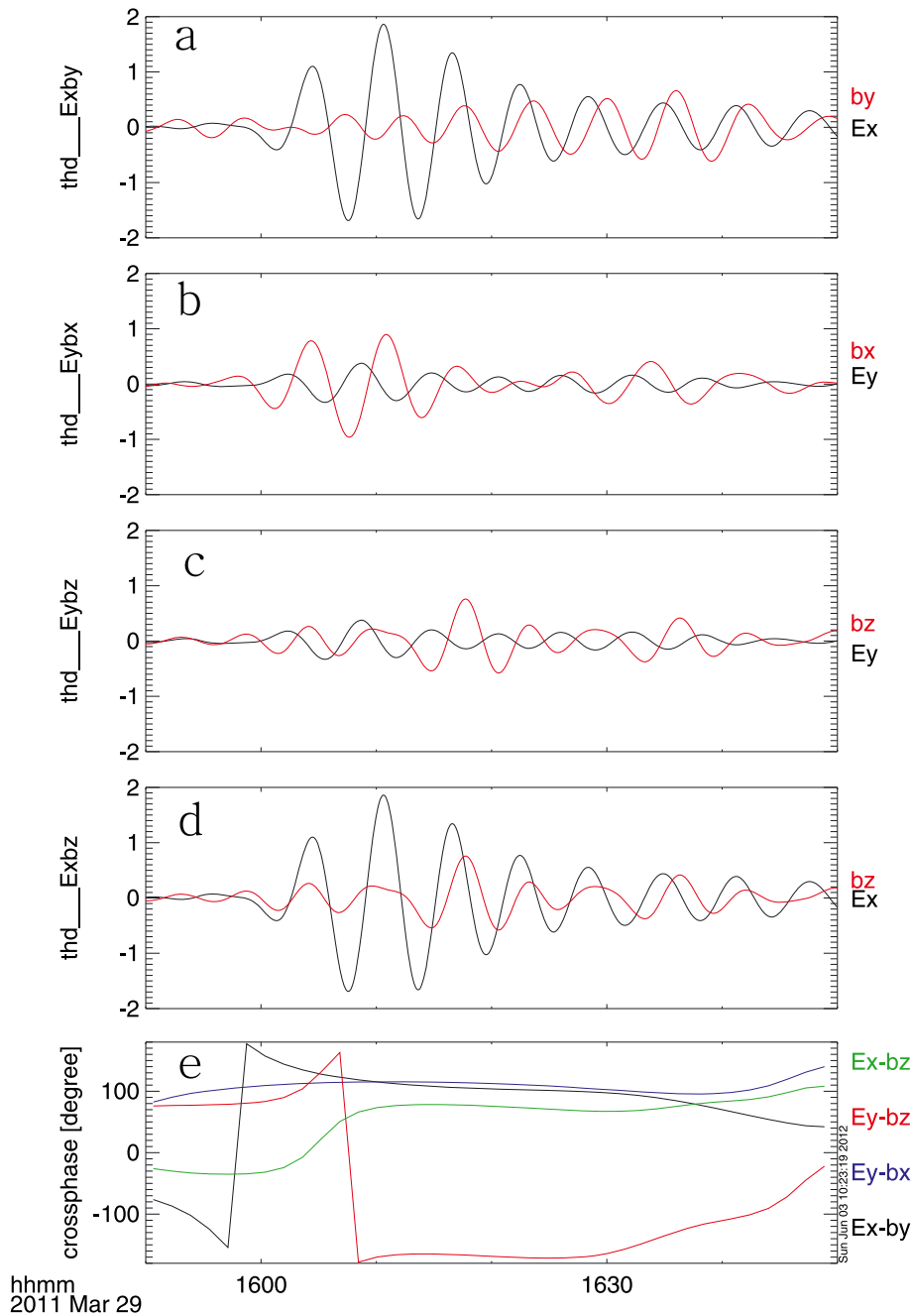


Figure 4. Field in field-aligned coordinates measured by THEMIS D and phase differences between magnetic and electric field components. (a) B_y - E_x , (b) E_x - B_y , (c) E_y - B_z , (d) E_x - B_z , and (e) phase difference between magnetic and electric field. The data have been band pass filtered in the range of 2.8 ± 1 mHz. Note that the large changes in phase seen in the bottom panel are due to wrap-around, i.e., the phase between E_x and B_y was changing gradually at 15:57 UT and did not abruptly increase by 360° .

possible scenario would be that the magnetopause was unstable before and after the pressure pulse, but a perturbation was required for the waves to grow to large amplitude (sufficiently large to be detected by THEMIS probes). Fluctuations in the magnetic field magnitude are one of the indicators of evanescent surface waves if we observe decaying amplitude with increasing distance from the magnetopause. However, for the cases examined here in which the probes were close together, decaying amplitude with increasing distance from the magnetopause

was not observed. Also, velocity shear at the magnetopause is an essential component of magnetopause surface wave growth via the Kelvin-Helmholtz instability, yet there was nothing exceptional about the velocity shear in the three cases out of 13 in which ULF waves were excited. In particular, the hourly averaged solar wind velocity, the dominant contributor to the shear flow, was in the range of 350–450 km/s for all three cases. Most of the events without ULF waves fell within or above this range; in two cases without waves,

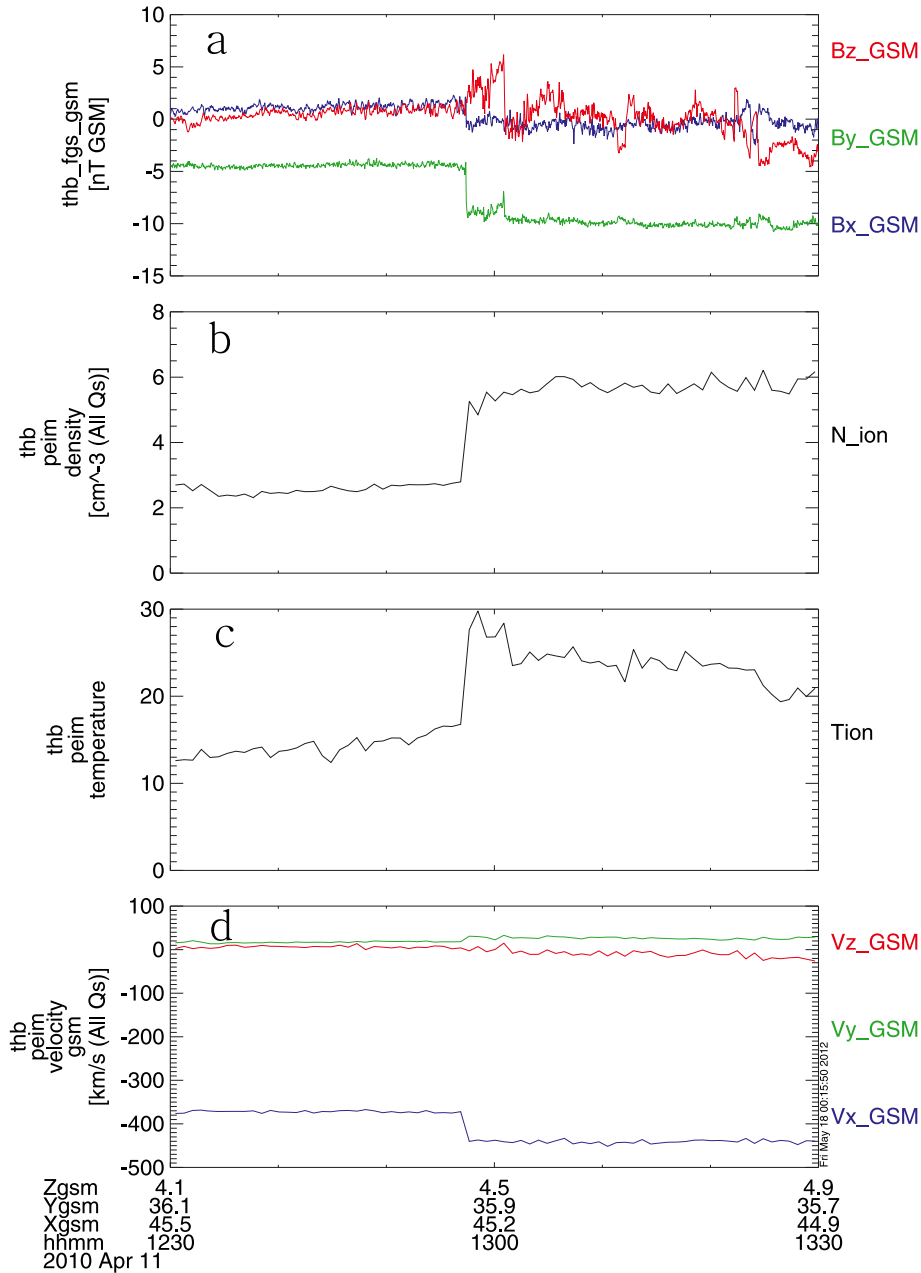


Figure 5. Themis B observations in the solar wind on 11 April 2010 (12:57 UT at (45.2, 36.0, 4.44) Re in GSM).

the solar wind flow speed was above 520 km/s. If the Kelvin-Helmholtz instability were the main explanation for the presence or absence of ULF wave activity, we would expect solar wind flow speed, which affects the growth rate of magnetopause surface waves, to be larger for events with wave activity. The absence of this relationship argues against the Kelvin-Helmholtz instability as the main mechanism for driving ULF waves following SI events. Furthermore, we found nothing exceptional about the orientation of the IMF (which also affects the Kelvin-Helmholtz stability of the magnetopause) in the three cases with ULF waves when compared to the other 10 cases. We conclude that surface waves driven by the Kelvin-Helmholtz instability are an unlikely source of ULF wave activity in these events.

[22] 2. Cavity/waveguide modes

When a solar wind pressure pulse compresses the magnetosphere, it generates compressional waves with a broadband frequency spectrum. A cavity mode [Kivelson and Southwood, 1985] or a waveguide mode [Walker et al., 1992; Rickard and Wright, 1994; 1995] can act as a frequency filter for these compressional waves, selecting only frequencies equal to the eigenfrequencies of the cavity or waveguide. These compressional waves with discrete frequencies can then transfer energy to Alfvén waves with the same frequencies. It was difficult to apply cavity/waveguide theory to our observations. We notice that the Ex perturbations (representative Alfvén wave activity-toroidal mode) for the three cases of clear ULF wave activity started immediately

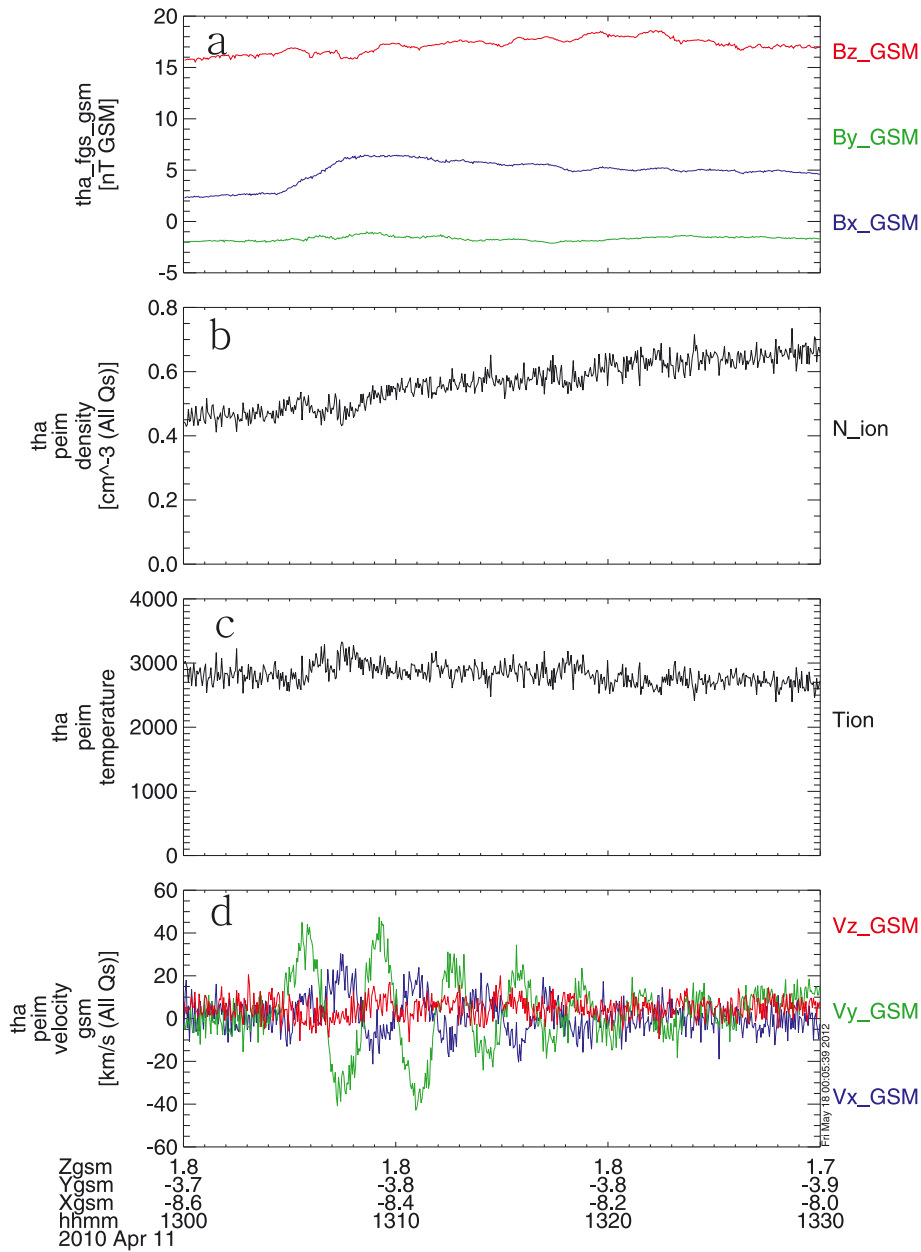


Figure 6. Themis A observations on 11 April 2010.

after the SI. If there were a cavity/waveguide mode providing energy to the Alfvén waves, normally some time would be required for energy transfer via FLR as modeled [Mann *et al.*, 1995] and observed in some cases [e.g., Eriksson *et al.*, 2006], and the Alfvén waves would grow gradually. In other words, after the pressure pulse first impinged on the magnetosphere, the global mode would be set up and appear first (if observable), while standing Alfvén waves would grow gradually over a few wave periods. In the events reported in section 2, however, the toroidal mode appears immediately and does not grow over several wave cycles.

Waveguide modes are excited during these SI events that may not be easily observed, either because of their low amplitudes or because they ought to have a broadband frequency spectrum in this region, since strong dispersion is expected as energy is transported down the tail [Rickard and Wright, 1995]. However,

these waveguide modes would not be expected to deposit much energy into standing Alfvén waves in the magnetotail, having expended much of the energy available for coupling in the dayside and flank magnetosphere [Rickard and Wright, 1994]. For these reasons, and the timescale of Alfvén wave growth mentioned above, we do not think that cavity/waveguide modes are important for determining the dominant (largest amplitude) ULF response of the magnetotail to SI events.

[23] 3. Direct excitation by a solar wind pressure pulse
A pressure pulse from the solar wind has a broadband frequency spectrum. A field line is expected to oscillate at its natural frequency in response to this broadband perturbation [e.g., Samson and Rostoker, 1972; Waters *et al.*, 1995]. In dayside SI events, standing Alfvén waves with a continuum of frequencies corresponding to the natural frequency of each field line have been observed [e.g., Sarris

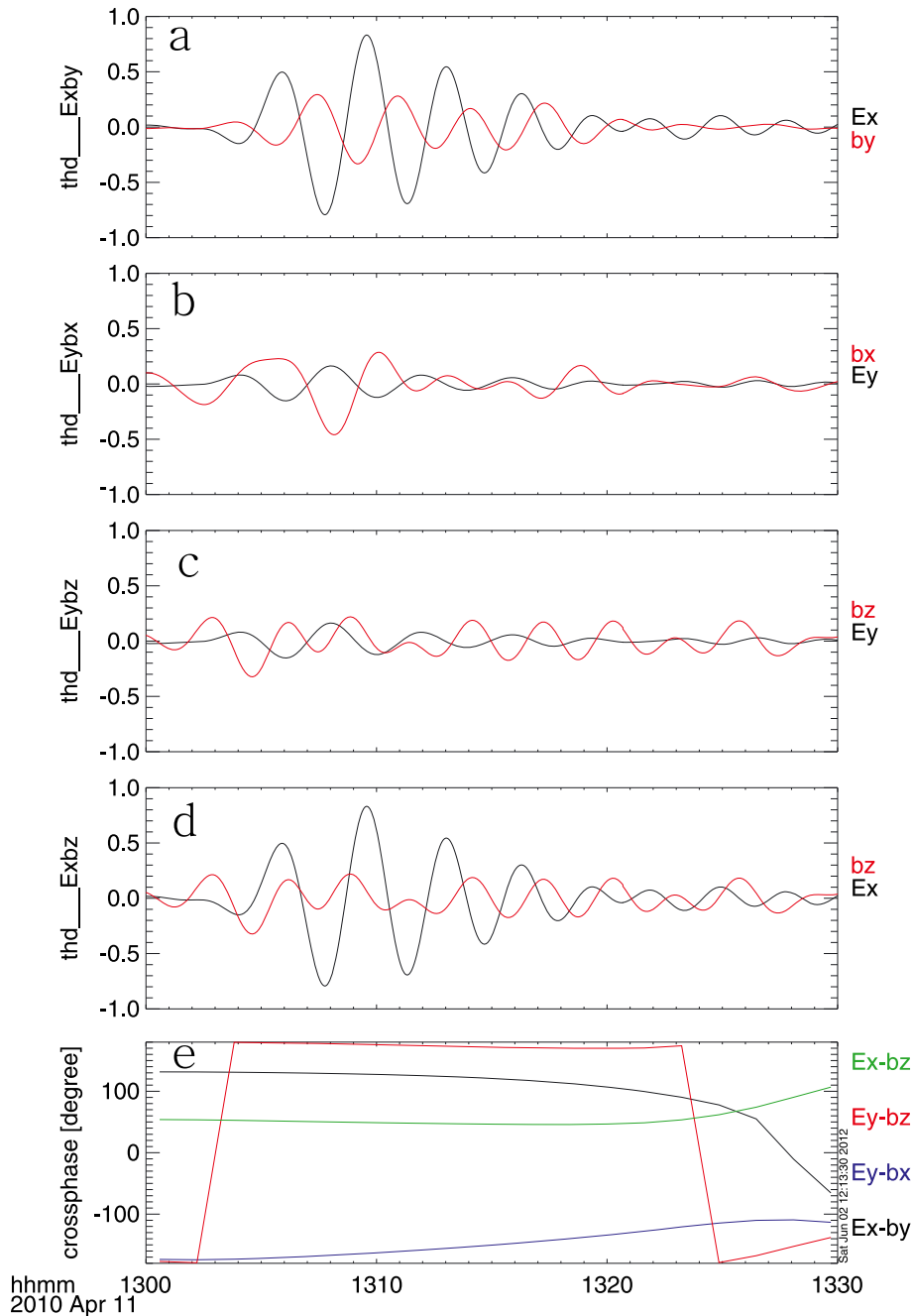


Figure 7. Same as Figure 4 but band pass filtered with pass band 4.5 ± 2 mHz on 11 April 2010.

et al., 2010]. In the three case studies presented in section 2, we do not observe a continuum of frequencies. However, there is only one case (24 April 2009) in which probes had large enough spatial separations to definitively show this; in this case, a probe did not observe significant wave activity that was located ~ 1 Re closer to the Earth than the probe that observed clear wave activity.

If Alfvén waves were directly excited by a source with a broadband frequency spectrum, we would have expected nearly all 13 SI events to have resulted in ULF wave activity. Since only 3 of 13 events have clear ULF wave activity and there are no events in which Alfvén waves with a continuum of frequencies are excited, we do not think that direct

excitation of Alfvén waves by a source with a broadband frequency spectrum is an important mechanism for driving ULF waves in the magnetotail during these SI events.

[24] 4. Solar wind-magnetotail force balance/magnetopause vortex

Sibeck [1990] proposed a model for the shock/magnetosphere interaction. In this model, a single or double vortex near the magnetopause can be generated when a shock passes through the magnetopause. When the change in dynamic pressure first impinges on the magnetosphere, a fast mode compressional wave is excited in the magnetosphere that generally propagates tailward faster than the solar wind. This causes the magnetopause to bulge outward ahead of the change in the solar

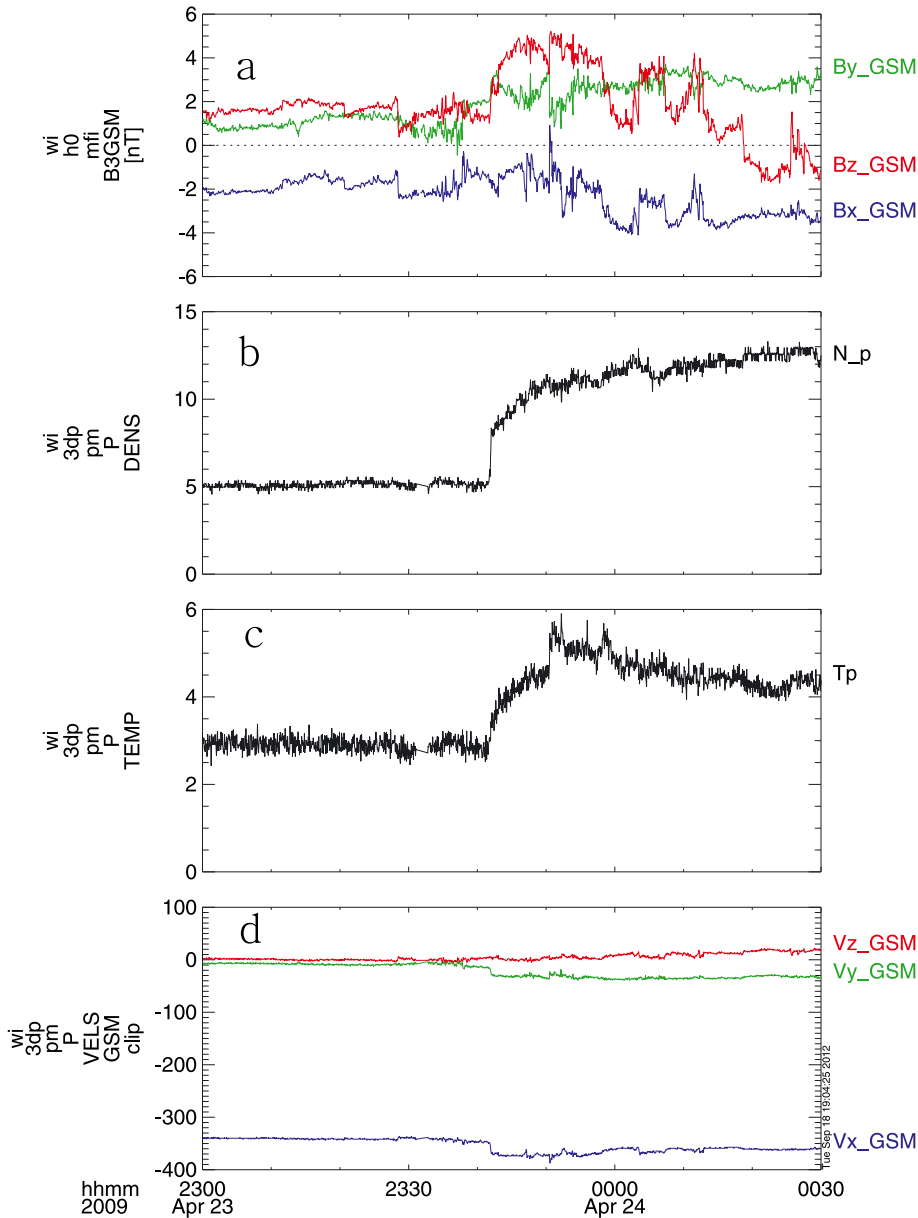


Figure 8. Wind observations in the solar wind on 23–24 April 2009.

wind dynamic pressure and inward once the solar wind perturbation compresses the magnetopause. These outward and inward bulges in turn create vortex structures inside the magnetosphere [Sibeck, 1990]. The properties of the magnetopause perturbations and vortices depend on both the strength of the solar wind pressure perturbation and the difference between the group velocity of magnetospheric fast mode waves and the solar wind velocity. This kind of vortex has previously been reported in the ionosphere from SuperDARN radar or ground magnetometers [e.g., Lyatsky *et al.*, 1999; Motoba *et al.*, 2003; Sibeck *et al.*, 2003; Juusola *et al.*, 2010]. In principle, these vortices can couple to standing shear Alfvén waves via FLR. The location and frequency of the standing Alfvén waves would be determined by the properties of the magnetopause perturbations/vortices. We have carried out a global MHD simulation through the Community Coordinated Modeling Center (CCMC) in which

we used the OpenGGCM MHD code [Raeder *et al.*, 2008] to run simulations of shock/magnetosphere interaction. In this simulation, the solar wind input data are set to be similar to those in our first event. The dipole tilt is set to be zero. The initial solar wind density is 4.0 n/cm^3 , while the temperature is $20,000.0 \text{ K}$ and velocity is $(-320, 0, 0) \text{ km/s}$ in GSE. The IMF is set to be $(0, 3, 3) \text{ nT}$ in GSE. When the shock arrives, the density, temperature, velocity and magnetic field changes to be 7 n/cm^3 , $30,000.0 \text{ K}$, $(-380, 0, 0) \text{ km/s}$, and $(0, 7, 5) \text{ nT}$ in GSE in 10 s. From the simulation results, we find that compression of the magnetopause launches a fast mode wave in the magnetosphere that propagates faster than the pressure pulse in the magnetosheath, as Sibeck [1990] predicted. For this reason, we find that the tailward flow enhancement due to the propagation of this fast wave is earlier (~ 2 mins—this is consistent with a calculation using observations from THEMIS B, C, and D) than the flow enhancement in the sheath. A

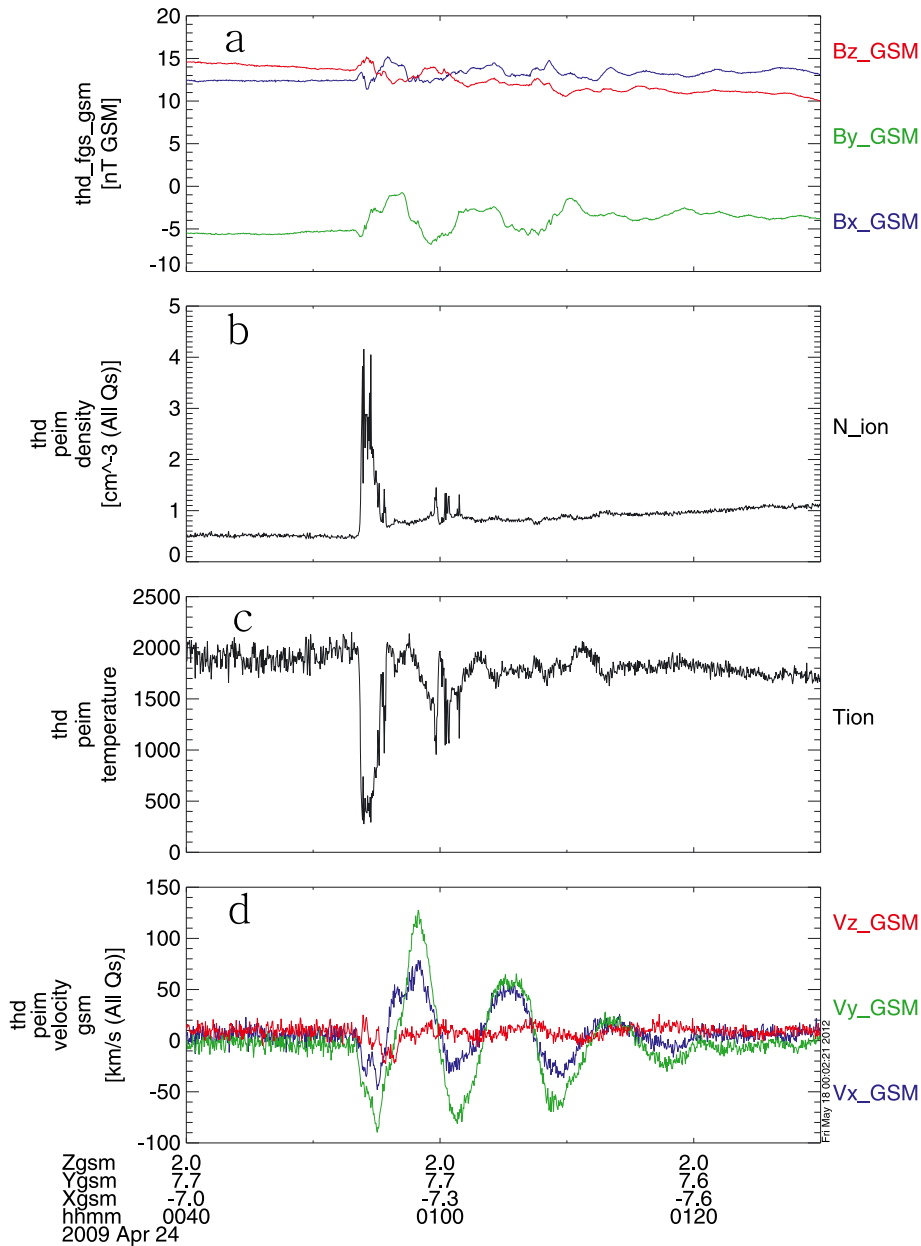


Figure 9. Themis D observations on 24 April 2009.

tailward-moving single vortex at the dawn and dusk side of the magnetopause can also be found in the simulation results, as shown in Figure 11, which is consistent with Sibeck' [1990] model. This kind of tailward-moving vortex is evident in one event (24 April 2009) from observation of three different probes (THEMIS B, C, and D) at different locations, which will be discussed in detail in another paper. In the positions at which the shock passes in the simulation box, we can find velocity vectors first tailward and then earthward, similar to our observed ULF wave signatures at the beginning of the SI event, although after the vortex passes this motion stops. The simulation results suggest that probes in the near Earth plasma sheet will see ULF wave signatures consistent with a shock-induced vortex during the early stages of shock passage. Later wave activity cannot be explained by the vortex. Standing Alfvén wave activity is not captured well by

MHD simulations, however, and our observations of later wave activity could be standing Alfvén waves driven by the vortex via FLR.

[25] The *Sibeck* [1990] model is an appealing explanation for the ULF response of the magnetotail to an SI for a number of reasons:

[26] 1. An MHD simulation of one of the events clearly demonstrates the presence of the vortex/magnetopause perturbation.

[27] 2. The velocity perturbations associated with the vortex can excite longer-lasting standing Alfvén wave activity via FLR.

[28] 3. The vortex may not be present or fully developed for all events (depending on the amplitude of solar wind dynamic pressure perturbation and the difference between the magnetospheric fast mode group velocity and solar wind

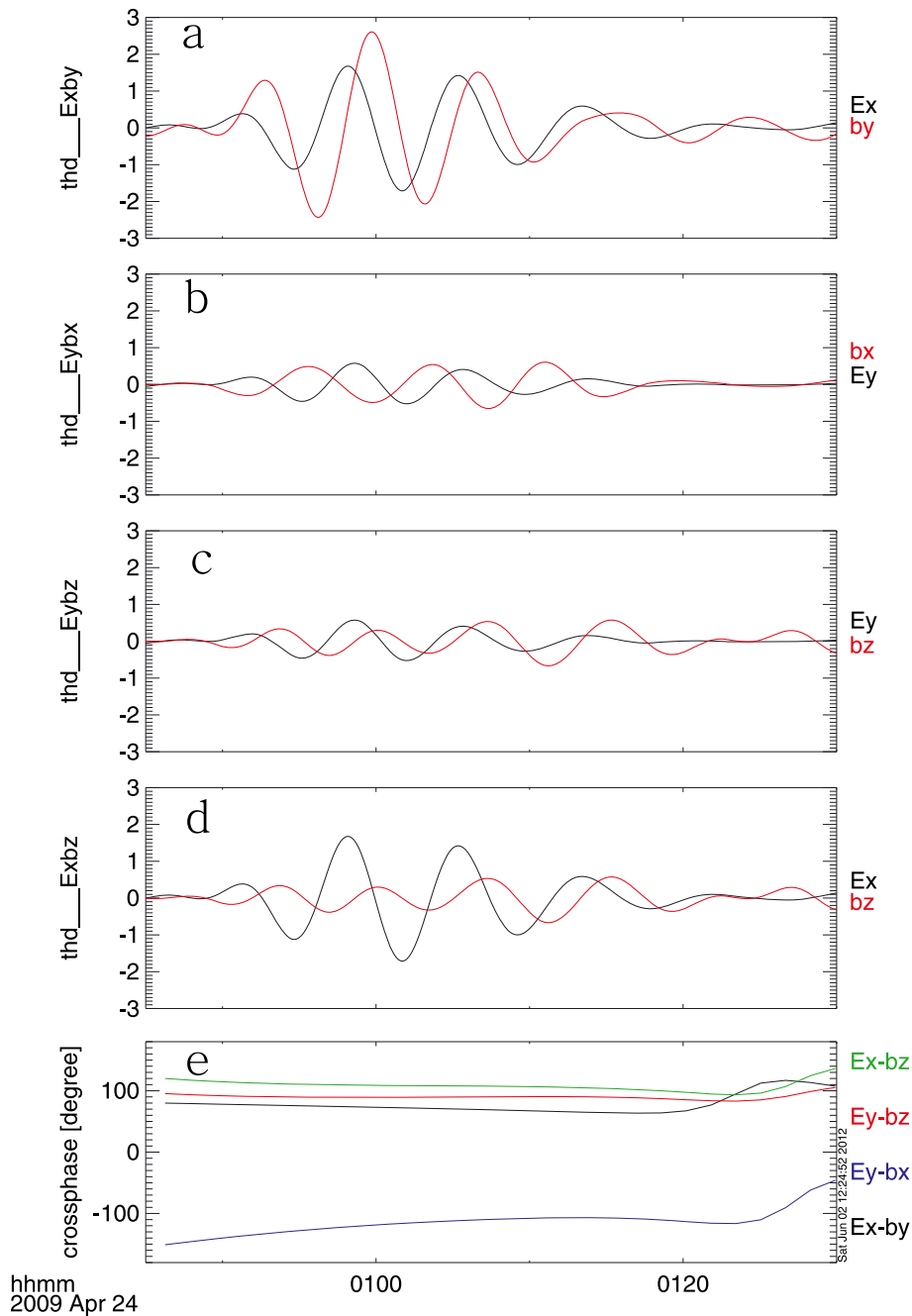


Figure 10. Same as Figure 4 but band pass filtered with pass band 2.2 ± 1 mHz on 24 April 2009.

velocity). This can partially explain why ULF wave activity was only observed in 3 of 13 SI events.

[29] 4. The vortex will only excite standing Alfvén waves at certain frequencies and locations, determined by the azimuthal phase velocity of the vortex [Wright and Rickard, 1995]. Furthermore, the signature of the vortex itself may only be apparent near the magnetopause. Thus, a probe must be properly positioned in the magnetotail in order to observe Alfvén wave activity related to the vortex. This can also partially explain why only 3 of 13 SI events had ULF wave activity: there may have been wave activity present, but the THEMIS probes were not appropriately positioned to observe it.

[30] The *Sibeck* [1990] model is particularly suitable for explaining the presence or absence of ULF waves near the flank magnetosphere (e.g., 29 March 2011 and 24 April 2009). However, using this model to explain the presence of wave activity near the central magnetotail (11 April 2010) requires an assumption that vortices are generated with scale lengths comparable to half of the cross-tail distance. We do not know if that is a realistic assumption as we are not aware of any studies placing limits on the cross-tail scale of these vortices. We can at least say that either these vortices extend very deep into the magnetotail in cases such as 11 April 2010 or another mechanism must be involved to excite waves deep in the magnetotail.

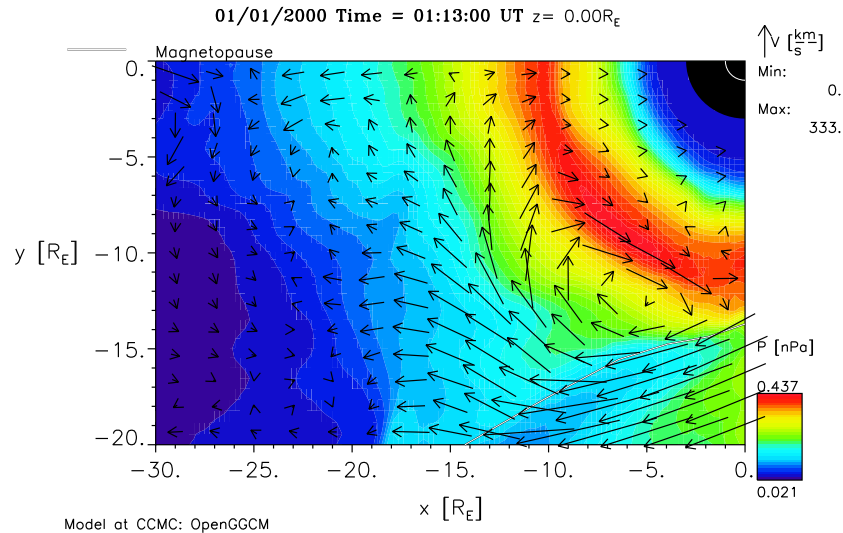


Figure 11. The CCMC simulation results in GSE. The background color indicates plasma pressure. The arrows represent the plasma vectors and the solid line marks the magnetopause position.

[31] These waves may be caused by another mechanism related to the force balance between the solar wind and the magnetotail. When the shock hits the magnetosphere, the compressional wave generated at the sub-solar point [e.g., *Sugiura et al.*, 1968; *Sibeck*, 1990] firstly causes the plasma to move tailward. Later, the magnetopause currents will be enhanced when the lateral pressure on the magnetopause in the tail increases [e.g., *Kawano et al.*, 1992; *Kim et al.*, 2004; *Huttunen et al.*, 2005]. The cross-tail current enhancement (due to the closure of stronger magnetopause currents) causes a $\mathbf{J} \times \mathbf{B}$ force on the tail plasma directed earthward, opposing the initial tailward plasma motion. Long duration wave activity may be set up via FLR if the timescale between the initial tailward push and later earthward push matches the natural frequency of the field line there. The advantage of this mechanism over the *Sibeck* [1990] model is that it could effectively drive ULF wave activity throughout the magnetotail rather than being restricted to locations near the magnetopause. As in the *Sibeck* [1990] model, the frequency and location of ULF waves resulting from the mechanism will depend on the difference between the velocity of fast mode waves in the magnetosphere and the solar wind velocity.

[32] We cannot unambiguously differentiate these two mechanisms using data from our observed ULF wave events. However, we can at least say that both can explain why only a small subset of SI events had observable ULF waves. Furthermore, the *Sibeck* [1990] model provides a ready explanation for initial wave activity for events with observations near the magnetopause.

[33] To summarize the results of this section, we considered several mechanisms that are typically used to explain the presence of ULF wave activity. After comparing with our observations, we found that only two mechanisms could explain the presence of ULF wave activity following SI events:

[34] 1. The Kelvin-Helmholtz instability cannot explain the presence or absence of ULF waves in the SI events considered in this study. Wave amplitudes are not observed to decrease with increasing distance from the magnetopause

and there is no clear relationship between velocity shear (solar wind flow speed)/IMF orientation and wave activity.

[35] 2. Cavity/waveguide modes cannot explain the presence or absence of ULF waves because Alfvén wave activity begins immediately after the passage of the SI and waves are excited in the magnetotail (remote from the location where waveguide modes would be expected to couple most effectively to Alfvén waves).

[36] 3. Solar wind pressure pulses cannot explain the presence or absence of ULF waves because multi-point observations did not reveal a continuum of Alfvén wave frequencies at different radial distances and ULF waves were only observed in 3 of 13 events.

[37] 4. A tailward-moving vortex, consistent with the *Sibeck* [1990] model, can explain the presence or absence of ULF waves in 3 of 13 events (although one event would require a vortex that extends deep into the tail) because it would involve a frequency selection (waves would only be observed when probes are appropriately positioned—otherwise, only a transient response would be observed), the vortex would not fully develop in all cases, and an MHD simulation for one event confirms the vortex as a valid explanation.

[38] 5. A dynamic response of the magnetotail to maintain force balance with the solar wind could also explain the presence or absence of ULF waves in 3 of 13 events, since it would also involve a frequency selection. We proposed this mechanism to explain ULF waves excited deep in the magnetotail for one SI event in particular; it is possible that a tailward-moving vortex could also have excited these waves, but a large vortex length scale would be required to achieve this.

4. Summary

[39] We studied the magnetotail response to interplanetary shocks or dynamic pressure enhancements in 13 events and found that ULF waves were excited in three events. These ULF wave events had perturbations consistent with toroidal modes that were likely excited by tailward moving vortices

predicted by the *Sibeck* [1990] model of the response of the magnetosphere to a dynamic pressure pulse or by the dynamic response of the magnetotail to maintain force balance with the solar wind. The operation of either of these mechanisms can explain why only 3 of 13 events had ULF wave activity. These mechanisms can also explain why steady ULF wave activity is not observed at all locations in the magnetotail during SI events.

[40] **Acknowledgments.** We acknowledge NASA THEMIS contract NAS5-02099; J. Bonnell and F. S. Mozer for use of the EFI data; and C. W. Carlson and J. P. McFadden for the use of the ESA data; and K. H. Glassmeier, U. Auster and W. Baumjohann for the use of FGM data provided under the lead of the Technical University of Braunschweig and with financial support through the German Ministry for Economy and Technology and the German Center for Aviation and Space (DLR) under contract 50 OC 0302. Simulation results have been provided by the Community Coordinated Modeling Center at Goddard Space Flight Center through their public Runs on Request system (<http://ccmc.gsfc.nasa.gov>). The CCMC is a multi-agency partnership between NASA, AFMC, AFOSR, AFRL, AFWA, NOAA, NSF, and ONR. The OpenGGCM was developed by Joachim Raeder and co-workers at the University of New Hampshire. We are grateful to FGM, CIS team for providing the Cluster data, CDAWeb for providing the WIND data, and Canadian Space Science Data Portal for providing the calculation of FLR frequency. The authors thank M. Kivelson, and T. S. Hsu for helpful discussions. We are grateful to Cindy Russell for help with software and Judy Hohl for help with editing. This work is supported by NNSFC 41031065, 41074106, the Shandong Natural Science Foundation JQ201112.

References

- Abraham-Shauner, B. (1972), Determination of magnetohydrodynamic shock normals, *J. Geophys. Res.*, *77*(4), 736–739, doi:10.1029/JA077i004p00736.
- Angelopoulos, V. (2008), The THEMIS Mission, *Space Sci. Rev.*, *141*, 5–34, doi:10.1007/s11214-008-9336-1.
- Auster, H. U., et al. (2008), The THEMIS fluxgate magnetometer, *Space Sci. Rev.*, *141*(1–4), 235–264.
- Balogh, A., et al. (2001), The cluster magnetic field investigation: Overview of in-flight performance and initial results, *Ann. Geophys.*, *19*(10–12), 1207–1217.
- Baumjohann, W., H. Junginger, G. Haerendel, and O. H. Bauer (1984), Resonant Alfvén waves excited by a sudden impulse, *J. Geophys. Res.*, *89*(A5), 2765–2769, doi:10.1029/JA089iA05p02765.
- Baumjohann, W., O. H. Bauer, G. Haerendel, H. Junginger, and E. Amata (1983), Magnetospheric plasma drifts during a sudden impulse, *J. Geophys. Res.*, *88*(A11), 9287–9289.
- Berube, D., M. B. Moldwin, and M. Ahn (2006), Computing magnetospheric mass density from field line resonances in a realistic magnetic field geometry, *J. Geophys. Res.*, *111*, A08206, doi:10.1029/2005JA011450.
- Cahill, L. J., Jr., N. G. Lin, J. H. Waite, M. J. Engebretson, and M. Sugiura (1990), Toroidal standing waves excited by a storm sudden commencement: DE 1 observations, *J. Geophys. Res.*, *95*(A6), 7857–7867, 829967, 828299.
- Chen, L., and A. Hasegawa (1974), A theory of long-period magnetic pulsations. I. Steady state excitation of field line resonance, *J. Geophys. Res.*, *79*(7), 1024–1032.
- Dungey, J. W. (1954), Electrodynamic of the outer atmosphere, Penn. State Univ. Ionos. Res. Lab. Sci. Rept.
- Dungey, J. W. (1963), Hydromagnetic waves and the ionosphere, in *Proceedings of the International Conference Held July, 1962 at Imperial College, London*, edited by A. C. Stickland, p. 230–280, Institute of Physics and the Physical Society, London.
- Eriksson, P. T. I., L. G. Blomberg, S. Schaefer, and K. H. Glassmeier (2006), On the excitation of ULF waves by solar wind pressure enhancements, *Ann. Geophys.*, *24*(11), 3161–3172.
- Farrell, W. M., R. F. Thompson, R. P. Lepping, and J. B. Byrnes (1995), A method of calibrating magnetometers on a spinning spacecraft, *IEEE Trans. Magn.*, *31*(2), 966–972.
- Glassmeier, K. H., C. Othmer, R. Cramm, M. Stellmacher, and M. Engebretson (1999), Magnetospheric field line resonances: A comparative planetology approach, *Surveys in Geophys.*, *20*(1), 61–109.
- Gloeckler, G., et al. (1995), The solar-wind and superthermal ion composition investigation on the wind spacecraft, *Space Sci. Rev.*, *71*(1–4), 79–124.
- Greenwald, R. A., and A. D. M. Walker (1980), Energetics of long period resonant hydromagnetic waves, *Geophys. Res. Lett.*, *7*(10), 745–748, doi:10.1029/GL007i010p00745.
- Hammond, C. M., M. G. Kivelson, and R. J. Walker (1994), Imaging the effect of dipole tilt on magnetotail boundaries, *J. Geophys. Res.*, *99*(A4), 6079–6092.
- Hartering, M., V. Angelopoulos, M. B. Moldwin, K.-H. Glassmeier, and Y. Nishimura (2011), Global energy transfer during a magnetospheric field line resonance, *Geophys. Res. Lett.*, *38*, L12101, doi:10.1029/2011GL047846.
- Huttunen, K. E. J., J. Slavin, M. Collier, H. E. J. Koskinen, A. Szabo, E. Tanskanen, A. Balogh, E. Lucek, and H. R. Reme (2005), Cluster observations of sudden impulses in the magnetotail caused by interplanetary shocks and pressure increases, *Ann. Geophys.*, *23*(2), 609–624.
- Juusola, L., K. Andreeva, O. Amm, K. Kauristie, S. E. Milan, M. Palmroth, and N. Partamies (2010), Effects of a solar wind dynamic pressure increase in the magnetosphere and in the ionosphere, *Ann. Geophys.*, *28*(10), 1945–1959.
- Kaufmann, R. L., and D. N. Walker (1974), Hydromagnetic waves excited during an ssc, *J. Geophys. Res.*, *79*(34), 5187–5195, doi:10.1029/JA079i034p05187.
- Kawano, H., T. Yamamoto, S. Kokubun, and R. P. Lepping (1992), Rotational properties of sudden impulses in the magnetotail lobe, *J. Geophys. Res.*, *97*(A11), 17,177–17,182.
- Kim, K.-H., C. A. Cattell, D.-H. Lee, A. Balogh, E. Lucek, M. Andre, Y. Khotyaintsev, and H. Rème (2004), Cluster observations in the magnetotail during sudden and quasiperiodic solar wind variations, *J. Geophys. Res.*, *109*, A04219, doi:10.1029/2003JA010328.
- Kivelson, M. G. (2006), ULF waves from the ionosphere to the outer planets, in *Magnetospheric ULF Waves: Synthesis and New Directions*, vol. 169, edited by K. Takahashi et al., pp. 11–30, AGU, Washington, D. C., doi:10.1029/169GM04.
- Kivelson, M. G., and D. J. Southwood (1985), Resonant ULF waves: A new interpretation, *Geophys. Res. Lett.*, *12*(1), 49–52, doi:10.1029/GL012i001p00049.
- Lui, A. T. Y., and C. Z. Cheng (2001), Resonance frequency of stretched magnetic field lines based on a self-consistent equilibrium magnetosphere model, *J. Geophys. Res.*, *106*(A11), 25,793–25,802.
- Lyatsky, W. B., G. J. Sofko, A. V. Kustov, D. Andre, W. J. Hughes, and D. Murr (1999), Traveling convection vortices as seen by the SuperDARN HF radars, *J. Geophys. Res.*, *104*(A2), 2591–2601.
- Mann, I. R., A. N. Wright, and P. S. Cally (1995), Coupling of magnetospheric cavity modes to field line resonances: A study of resonance widths, *J. Geophys. Res.*, *100*(A10), 19,441–19,456.
- McFadden, J. P., C. W. Carlson, D. Larson, M. Ludlam, R. Abiad, B. Elliott, P. Turin, M. Marckwordt, and V. Angelopoulos (2008), The THEMIS ESA plasma instrument and in-flight calibration, *Space Sci. Rev.*, *141*(1–4), 277–302.
- McPherron, R. (2005), Magnetic pulsations: Their sources and relation to solar wind and geomagnetic activity, *Surv. Geophys.*, *26*(5), 545–592.
- Motoba, T., T. Kikuchi, T. Okuzawa, and K. Yumoto (2003), Dynamical response of the magnetosphere-ionosphere system to a solar wind dynamic pressure oscillation, *J. Geophys. Res.*, *108*(A5), 1206–1216, doi:10.1029/2002JA009696.
- Nopper, R. W., Jr., W. J. Hughes, C. G. MacLennan, and R. L. McPherron (1982), Impulse-excited pulsations during the July 29, 1977, event, *J. Geophys. Res.*, *87*(A8), 5911–5916, doi:10.1029/JA087iA08p05911.
- Rae, I. J., C. E. J. Watt, F. R. Fenrich, I. R. Mann, L. G. Ozeke, and A. Kale (2007), Energy deposition in the ionosphere through a global field line resonance, *Ann. Geophys.*, *25*(12), 2529–2539.
- Raeder, J., D. Larson, W. H. Li, E. L. Kepko, and T. Fuller-Rowell (2008), OpenGGCM simulations for the THEMIS mission, *Space Sci. Rev.*, *141*(1–4), 535–555.
- Rankin, R., F. Fenrich, and V. T. Tikhonchuk (2000), Shear Alfvén waves on stretched magnetic field lines near midnight in Earth’s magnetosphere, *Geophys. Res. Lett.*, *27*(20), 3265–3268.
- Reme, H., et al. (2001), First multispacecraft ion measurements in and near the Earth’s magnetosphere with the identical Cluster ion spectrometer (CIS) experiment, *Ann. Geophys.*, *19*(10–12), 1303–1354.
- Rickard, G. J., and A. N. Wright (1994), Alfvén resonance excitation and fast wave propagation in magnetospheric waveguides, *J. Geophys. Res.*, *99*(A7), 13,001–13,010, doi:10.1029/99JA00703.
- Rickard, G. J., and A. N. Wright (1995), ULF pulsations in a magnetospheric wave guide comparison of real and simulated satellite data, *J. Geophys. Res.*, *100*(A3), 3531–3537.
- Russell, C. T., M. M. Mellott, E. J. Smith, and J. H. King (1983), Multiple spacecraft observations of the interplanetary shocks: Four spacecraft determination of shock normals, *J. Geophys. Res.*, *88*(NA6), 4739–4748.
- Samson, J. C., and G. Rostoker (1972), Latitude-dependent characteristics of high-latitude Pc 4 and Pc 5 micropulsations, *J. Geophys. Res.*, *77*(31), 6133–6144, doi:10.1029/JA077i031p06133.
- Samson, J. C., L. L. Cogger, and Q. Pao (1996), Observations of field line resonances, auroral arcs, and auroral vortex structures, *J. Geophys. Res.*, *101*(A8), 17,373–17,383, doi:10.1029/96JA01086.

- Sarafopoulos, D. V., and E. T. Sarris (1994), Quiet-time PC-5 pulsations in the earth's magnetotail—IMF-8, ISEE-1 and ISEE-3 simultaneous observations, *Ann. Geophys.-Atmos. Hydrospheres and Space Sci.*, *12*(2–3), 121–138.
- Sarris, T. E., W. Liu, X. Li, K. Kabin, E. R. Talaat, R. Rankin, V. Angelopoulos, J. Bonnell, and K. H. Glassmeier (2010), THEMIS observations of the spatial extent and pressure-pulse excitation of field line resonances, *Geophys. Res. Lett.*, *37*, L15104, doi:10.1029/2010GL044125.
- Sibeck, D. G. (1990), A model for the transient magnetospheric response to sudden solar wind dynamic pressure variations, *J. Geophys. Res.*, *95*(A4), 3755–3771, doi:10.1029/JA095iA04p03755.
- Sibeck, D. G., N. B. Trivedi, E. Zesta, R. B. Decker, H. J. Singer, A. Szabo, H. Tachihara, and J. Watermann (2003), Pressure-pulse interaction with the magnetosphere and ionosphere, *J. Geophys. Res.*, *108*(A2), 1095, doi:10.1029/2002JA009675.
- Southwood, D. J. (1974), Some features of field line resonances in the magnetosphere, *Planet. Space Sci.*, *22*(3), 483–491.
- Southwood, D. J., and M. G. Kivelson (1981), Charged particle behavior in low-frequency geomagnetic pulsations. I. Transverse waves, *J. Geophys. Res.*, *86*(A7), 5643–5655.
- Southwood, D. J., and W. J. Hughes (1983), Theory of hydromagnetic waves in the magnetosphere, *Space Sci. Rev.*, *35*(4), 301–366.
- Southwood, D. J., and M. G. Kivelson (1990), The magnetohydrodynamic response of the magnetospheric cavity to changes in solar wind pressure, *J. Geophys. Res.*, *95*(A3), 2301–2309, doi:10.1029/JA095iA03p02301.
- Sugiura, M., T. Skillman, B. Ledley, and J. Heppner (1968), Propagation of the sudden commencement of July 8, 1966, to the magnetotail, *J. Geophys. Res.*, *73*(21), 6699–6709.
- Tian, A. M., et al. (2012), Dynamics of long-period ULF waves in the plasma sheet: Coordinated space and ground observations, *J. Geophys. Res.*, *117*, A03211, doi:10.1029/2011JA016551.
- Walker, A. D. M., J. M. Ruohoniemi, K. B. Baker, and R. A. Greenwald (1992), Spatial and temporal behavior of ULF pulsations observed by the Goose Bay HF radar, *J. Geophys. Res.*, *97*(A8), 12,187–12,202.
- Waters, C. L., J. C. Samson, and E. F. Donovan (1995), The temporal variation of the frequency of high-latitude field line resonances, *J. Geophys. Res.*, *100*(A5), 7987–7996.
- Wedeken, U., B. Inhester, A. Korth, K.-H. Glassmeier, R. Gendrin, L. J. Lanzerotti, H. Gough, C. A. Green, E. Amata, A. Pedersen and G. Rostoker (1984), Ground-satellite coordinated study of the April 5, 1979 events: Flux variations of energetic particles and associated magnetic pulsations, *J. Geophys. Res.*, *89*, 120–133.
- Wilken, B., C. K. Goertz, D. N. Baker, P. R. Higbie, and T. A. Fritz (1982), The SSC on July 29, 1977 and its propagation within the magnetosphere, *J. Geophys. Res.*, *87*(A8), 5901–5910, doi:10.1029/JA087iA08p05901.
- Wright, A. N., and G. J. Rickard (1995), A numerical study of resonant absorption in a magnetohydrodynamic cavity driven by a broad-band spectrum, *Astrophys. J.*, *444*(1), 458–470.
- Yao, L., P. B. Zuo, X. S. Feng, and Z. X. Liu (2010), Responses of the magnetotail plasma sheet to two interplanetary shocks: TC-1 observations, *Chin. Sci. Bull.*, *55*(6), 530–538.
- Zhang, X. Y., Q. G. Zong, Y. F. Wang, H. Zhang, L. Xie, S. Y. Fu, C. J. Yuan, C. Yue, B. Yang, and Z. Y. Pu (2010), ULF waves excited by negative/positive solar wind dynamic pressure impulses at geosynchronous orbit, *J. Geophys. Res.*, *115*, A10221, doi:10.1029/2009JA015016.
- Zheng, Y., et al. (2006), Coordinated observation of field line resonance in the mid-tail, *Ann. Geophys.*, *24*(2), 707–723.
- Zong, Q.-G., X.-Z. Zhou, Y. F. Wang, X. Li, P. Song, D. N. Baker, T. A. Fritz, P. W. Daly, M. Dunlop, and A. Pedersen (2009), Energetic electron response to ULF waves induced by interplanetary shocks in the outer radiation belt, *J. Geophys. Res.*, *114*, A10204, doi:10.1029/2009JA014393.